Fluorescence Determination of Tryptophan Side-Chain Accessibility and Dynamics in Triple-Helical Collagen-Like Peptides

Kristine V. Simon-Lukasik,* Anton V. Persikov,† Barbara Brodsky,† John A. M. Ramshaw,‡ William R. Laws,§ J. B. Alexander Ross,§ and Richard D. Ludescher*

*Department of Food Science, Rutgers University, New Brunswick, New Jersey 08901; †Department of Biochemistry, Robert Wood Johnson Medical School–UMDNJ, Piscataway, New Jersey 08854; ‡CSIRO, 343 Royal Parade, Parkville, Victoria 3052, Australia; and §Department of Chemistry, University of Montana, Missoula, Montana 59812

ABSTRACT We report tryptophan fluorescence measurements of emission intensity, iodide quenching, and anisotropy that describe the environment and dynamics at X and Y sites in stable collagen-like peptides of sequence $(Gly\text{-}X\text{-}Y)_n$. About 90% of tryptophans at both sites have similar solvent exposed fluorescence properties and a lifetime of 8.5–9 ns. Analysis of anisotropy decays using an associative model indicates that these long lifetime populations undergo rapid depolarizing motion with a 0.5 ns correlation time; however, the extent of fast motion at the Y site is considerably less than the essentially unrestricted motion at the X site. About 10% of tryptophans at both sites have a shorter (~3 ns) lifetime indicating proximity to a protein quenching group; these minor populations are immobile on the peptide surface, depolarizing only by overall trimer rotation. Iodide quenching indicates that tryptophans at the X site are more accessible to solvent. Side chains at X sites are more solvent accessible and considerably more mobile than residues at Y sites and can more readily fluctuate among alternate intermolecular interactions in collagen fibrils. This fluorescence analysis of collagen-like peptides lays a foundation for studies on the structure, dynamics, and function of collagen and of triple-helical junctions in gelatin gels.

INTRODUCTION

The triple helix folding motif occurs in the fibrillar collagens of bone, tendon, skin, and cartilage, in more than 15 types of nonfibrillar collagens (Kielty et al., 1993) and in noncollagenous host-defense proteins (Hoppe and Reid, 1994). The triple helix consists of three supercoiled, polyproline II-like chains (Rich and Crick, 1961; Bella et al., 1994) with a repeating sequence of $(Gly\text{-}X\text{-}Y)_n$ in which Pro and Hyp often occupy the X and Y sites. Buried Gly residues form a closely packed core that prevents substitution by any larger residue without helix distortion. In contrast, residues in the nonequivalent X and Y sites are largely accessible to solvent (Jones and Miller, 1991; Kramer et al., 2001); any residue can occupy these sites (Rich and Crick, 1961; Persikov et al., 2000).

Synthetic peptides have provided insight into the molecular structure, thermodynamic stability, and folding kinetics of the triple helix (Baum and Brodsky, 1999). Gly-X-Y peptides with a high content of Pro and Hyp adopt a triple helix amenable to x-ray crystallography (Bella et al., 1994; Kramer et al., 2001) and multidimensional NMR (Buevich and Baum, 2001). Recent studies of host-guest triple-helical peptides where one Gly-X-Y triplet is embedded in seven stabilizing Gly-Pro-Hyp triplets (Persikov et al., 2000) have established a propensity scale for the 20 common residues in the X and Y sites. Although all peptides formed stable triple helices, those with aromatic residues at either the X or Y sites were the least stable.

Studies of intrinsic fluorescence in the collagen triple helix offer an opportunity to characterize the mobility and accessibility of individual side chains at X and Y sites and to relate them to biological function. Intrinsic fluorescence studies of the abundant fibril forming collagens have been limited by the absence of Trp and scarcity of Tyr in their triple-helical domains. When these aromatic amino acids are present, fluorescence has been used to detect cross-links formed between Tyr and Phe (Fujimori, 1966; Menter et al., 1995). Synthetic peptides with N-terminal Trp have been used as energy transfer probes of collagenase cleavage (Muller et al., 2000). In an elegant study, Golbik and coworkers (2000) used energy transfer from Phe to a unique Trp in the integrin binding domain of type IV heterotrimeric collagen to investigate the topology between the $\alpha1'\alpha1\alpha2$ chains. In general, however, fluorescence has primarily been used to study collagen cross-links associated with age and diabetes (Sell et al., 1991; Uebelhart and Delmas, 1993).

To demonstrate that intrinsic protein fluorescence can be used to investigate collagen structure, dynamics, and function, we have assessed the steady-state and time-resolved fluorescence properties of two triple-helical host-guest synthetic peptides with Trp at either the X or the Y site. These studies highlight the similarities in the water-exposed local environment and molecular dynamics at these sites in the collagen triple helix, but also reveal that the Trp side chain at the X site is more solvent accessible and has considerably greater mobility than Trp at the Y site.

Submitted June 26, 2002, and accepted for publication August 21, 2002.

Address reprint requests to Richard D. Ludescher, Dept. of Food Science, 65 Dudley Road, New Brunswick, NJ 08901-8520. Tel.: 732-932-9611 ext. 231; Fax: 732-932-6776; E-mail: ludescher@aesop.rutgers.edu.

Abbreviations used: Hyp, hydroxyproline; GWO, peptide with Trp at X site; GPW, peptide with Trp at Y site; NATA, *N*-acetyl-tryptophanamide.

0006-3495/03/01/501/08 $2.00

MATERIALS AND METHODS

Sample preparation

The peptides Ac-(Gly-Pro-Hyp)$_3$-Gly-Trp-Hyp-(Gly-Pro-Hyp)$_4$-Gly-Gly-$CONH_2$, GWO, and Ac-(Gly-Pro-Hyp)$_3$-Gly-Pro-Trp-(Gly-Pro-Hyp)$_4$-Gly-Gly-$CONH_2$, GPW, were synthesized by solid-phase chemistry and purified as described (Persikov et al., 2000). Laser desorption mass spectrometry (MALDI) confirmed peptide identity; the masses of trimeric GWO and GPW were 7203 Da and 7155 Da, respectively. Peptides were dried for 48 h before weighing and dialyzed against phosphate-buffered saline (PBS) (0.15 M NaCl, 20 mM sodium phosphate, pH 7.0). Peptide concentrations were determined from the absorption at 280 nm using an extinction coefficient for Trp of 5690 $M^{-1}cm^{-1}$ (Edelhoch, 1967). Before use, peptide solutions were held at 5°C for >48 h to ensure complete triple-helix formation; all spectroscopic measurements were done at 15°C. Purified peptides were dissolved at 1 mg/mL in PBS; any further dilutions of peptide were also made with PBS. All chemicals were from Sigma Chemical Co. (St. Louis, MO) and used without further purification.

Fluorescence emission

Fluorescence measurements were made using a SPEX Model F1T11I running Datamax software and the GRAMS/32 data processing module (Jobin Yvon, Inc., Edison, NJ) and equipped with Glan-Thompson polarizers on excitation and emission when appropriate. Fluorescence measurements were made at right angle in a 10-mm × 2-mm dual path length quartz cuvette; background fluorescence from buffer was negligible.

Fluorescence emission spectra for relative quantum yields were measured (1-nm increment, 5.6-nm bandpass, 5-s integration time) using 280-nm excitation. Three emission spectra for each peptide were integrated over 295–500 nm; the average area (S) and A_{280} values of the GPW and GWO peptides were used to calculate the ratio of quantum yields (Q):

$$Q_{GPW}/Q_{GWO} = (S/A_{280})_{GPW}/(S/A_{280})_{GWO} \quad (1)$$

Fluorescence quenching

Stern-Volmer quenching was performed using 280-nm excitation and 355-nm emission. Iodide stock solutions (1 M KI in PBS) were made fresh before use, held on ice, and protected from light. One-minute averaged fluorescence intensities were corrected for dilution and iodide absorption at 280 nm and plotted as the ratio of initial fluorescence intensity (F_o) to intensity (F) at each quencher concentration (F_o/F vs. [Q].) The slope determined by linear regression was K_{sv}, the Stern-Volmer quenching constant; average values of K_{sv} for each peptide were used in further calculations. The collisional quenching constant, k_q, is K_{sv} / $\langle\tau\rangle$, where $\langle\tau\rangle$ is the intensity average fluorescence lifetime (Table 1).

Fluorescence anisotropy

Steady-state anisotropy was measured using 280-nm excitation (7.6-nm bandpass); emission was collected in L format at 355 nm (11.4-nm bandpass). Intensities with excitation polarization either Vertical (V) or Horizontal (H) and emission polarization either V or H (I_{VV}, I_{VH}, I_{HH}, and I_{HV}) were collected and anisotropy (r) was calculated by the software module of the SPEX fluorimeter. Anisotropy values are the average of 15–20 measurements.

Data for Perrin plots were collected in T format with 280-nm excitation (11.4-nm bandpass) and 355-nm emission (30.4-nm bandpass). Solution viscosity was varied by addition of aliquots of a 66% w/w sucrose solution in PBS; background fluorescence from sucrose was negligible. Anisotropy values are reported as the average of 10 measurements. Viscosities at 15°C for each mass fraction of sucrose were determined using an Internet-based calculator (http://www.univ-reims.fr/Externes/AVH/MementoSugar/001.htm). Data were analyzed using the Perrin equation for an isotropic rotor:

$$1/r = 1/r_o + (\tau k_B/V_h r_o)(T/\eta), \quad (2)$$

where r_o is the intrinsic anisotropy in the absence of motion, V_h is the hydrodynamic volume, η is the viscosity, and k_B is the Boltzmann constant. The V_h of each triple-helical peptide was calculated from the slope determined by linear regression of the Perrin plot using the r_o value determined from the abscissa intercept and the intensity average lifetime ($\langle\tau\rangle$).

Time-resolved fluorescence

Fluorescence decay curves were collected using time-correlated single-photon counting. Thermostated samples in an automated sample chamber (FLASC1000, Quantum Northwest, Spokane, WA) were excited at 4.8 MHz with ~2-ps wide pulses (full-width-half-maximum) of the wavelength (280 or 295 nm) and vertical polarization generated by a laser system (Verdi V10, Mira 900, and pulse picker 9200 from Coherent, Santa Clara, CA; harmonic generator 5-050 from Inrad, Northvale, NJ). Emitted photons were selected for the desired polarization, and then passed through a monochromator (SpectraPro-150 from Acton Research, Acton, MA) set at 355 nm (10-nm bandpass) before detection by a photomultiplier tube module (TBX-04 from IBH, Glasgow, UK) containing a preamplifier and a constant fraction discriminator. Electronics (time-to-amplitude converter 566 and multichannel buffer 921E from EG&G Ortec, Oak Ridge, TN) processed the time between an excitation and emission event to collect a decay probability histogram over 2048 channels at 24 ps/channel. Instrument response functions (light scatter) and decay curves were typically collected to 100,000 and 40,000 peak counts, respectively; $I_M(t)$, $I_V(t)$, and $I_H(t)$ decay curves (see below) consisted of ~1.4×10^7, 1.2×10^7, and 1.5×10^7 total counts, respectively, for GWO samples, and 1.6×10^7, 1.4×10^7, and 1.6×10^7 total counts, respectively, for GPW samples.

Anisotropy decay data analysis

Fluorescence intensity decays, $I_M(t)$, were obtained under magic angle conditions (Badea and Brand, 1979) and defined as sums of exponentials:

$$I_M(t) = \frac{1}{3}\sum_{i=1}^{n} \alpha_i e^{-t/\tau_i} \quad (3)$$

We assume that each exponential component arises from an independent emitting state and that excited-state reactions or interactions do not occur, consistent with the rotamer model of Trp fluorescence in proteins in which the rotamers interconvert much slower than the excited state decay (Szabo and Rayner, 1980; Ross et al., 1992; McLaughlin and Barkley, 1997). Each τ_i term represents the lifetime of an individual emitting species and the preexponential α_i values depend on concentrations, extinction coefficients, and emission spectra of the species, as well as instrument parameters.

The anisotropy decay, $r(t)$, is related to the decays collected with vertical, $I_V(t)$, and horizontal, $I_H(t)$, polarization:

$$I_V(t) = I_M(t)\{1 + 2r(t)\} \quad (4)$$

$$I_H(t) = I_M(t)\{1 - r(t)\} \quad (5)$$

The anisotropy decay of a sample consists of the anisotropy decay of each emitting species, $r_i(t)$. As defined in Eq. 6, each $r_i(t)$ can be a sum of exponentials where the preexponential terms β_{ij} denote the extent to which each emitting species is depolarized by the various motions and the ϕ_j represent the rotational correlation times:

$$r_i(t) = \sum_{j=1}^{m} \beta_{ij} e^{-t/\phi_j} \quad (6)$$

TABLE 1 Fluorescence decay analysis results of Trp-containing collagen samples*

Sample	α_1†	α_2†	τ_1 (ns)§	τ_2 (ns)§	f_1¶	f_2¶	$\langle\tau\rangle$ (ns)‖	$\bar{\tau}$ (ns)**	χ^2††
GWO_1	0.113	0.887	2.43	8.36	3.6	96.4	8.12	7.18	1.024
	(0.107–0.118)§§	(0.885–0.889)	(2.32–2.54)	(8.35–8.37)					
GWO_2	0.113	0.887	2.35	8.36	3.5	96.5	8.12	7.14	1.061
	(0.107–0.119)	(0.882–0.891)	(2.16–2.56)	(8.34–8.37)					
GPW_1	0.155	0.845	2.93	9.08	5.6	94.4	8.71	7.68	1.009
	(0.149–0.161)	(0.843–0.847)	(2.84–3.03)	(9.07–9.10)					
GPW_2	0.137	0.863	2.87	9.09	4.8	95.2	8.77	7.80	1.031
	(0.135–0.140)	(0.862–0.864)	(2.81–2.93)	(9.08–9.10)					

Sample	β_{11}¶¶	β_{12}¶¶	β_{21}‖‖	β_{22}‖‖	ϕ_1 (ns)***	ϕ_2 (ns)***	$r_{0,1}$†††	$r_{0,2}$†††
GWO_1	0	0.332	0.098	0.014	0.57	11.4	0.332	0.112
		(0.290–0.376)	(0.090–0.105)	(0.012–0.016)	(0.52–0.63)	(8.1–17.5)		
GWO_2	0	0.356	0.103	0.014	0.52	15.6	0.356	0.116
		(0.266–0.436)	(0.094–0.112)	(0.007–0.020)	(0.44–0.62)	(9.9–23.4)		
GPW_1	0	0.331	0.073	0.060	0.46	10.5	0.331	0.134
		(0.310–0.351)	(0.065–0.082)	(0.058–0.062)	(0.36–0.56)	(9.5–11.6)		
GPW_2	0	0.354	0.065	0.064	0.49	10.0	0.354	0.128
		(0.334–0.374)	(0.056–0.073)	(0.062–0.066)	(0.41–0.58)	(9.5–10.6)		

*Decays obtained with excitation and fluorescence detection at 295 and 355 nm, respectively.
†Recovered amplitudes normalized to a sum of one.
§Recovered fluorescence intensity decay lifetimes.
¶Percent contribution to total emission; $f_i = 100\ \alpha_i\tau_i/\Sigma\alpha_i\tau_i$.
‖Intensity average lifetime: $\langle\tau\rangle = \Sigma\alpha_i\tau_i^2/\Sigma\alpha_i\tau_i$.
**Number average lifetime: $\bar{\tau} = \Sigma\alpha_i\tau_i/\Sigma\alpha_i$.
††The reduced, weighted sum of residuals for the anisotrophy dataset.
§§95% confidence interval.
¶¶Beta term recovered for the species having a lifetime of τ_1.
‖‖Beta term recovered for the species having a lifetime of τ_2.
***Recovered rotational correlation time.
†††Limiting anisotrophy recovered for the species having a liftetime of τ_1 or τ_2.

The sum of the β_{ij} values over all depolarizing motions for each emitting species provides the limiting anisotropy, r_{oi}, for that species.

In general, the total anisotropy decay is:

$$r(t) = \frac{\sum_{i=1}^{n}\left\{\alpha_i\, e^{-t/\tau_i}\sum_{j=1}^{m}\beta_{ij}\, e^{-t/\phi_j}\right\}}{\sum_{i=1}^{n}\alpha_i\, e^{-t/\tau_i}} \qquad (7)$$

Whereas it is generally assumed that *each* fluorophore is subject to *all* of the depolarizing motions, use of Eq. 7 permits unique lifetime-correlation time associations through independent β_{ij} values. For example, if a β_{ij} term equals zero, the species with lifetime τ_i is *not* depolarized by the motion leading to correlation time ϕ_j. Details have been published previously (Bialik et al., 1998; Rachofsky and Laws, 2000).

An anisotropy dataset of $I_M(t)$, $I_V(t)$, and $I_H(t)$ curves for a sample were analyzed simultaneously (globally) to recover the intensity and anisotropy decay parameters directly (Waxman et al., 1993) instead of fitting generated sum, difference or anisotropy curves with associated problems of parameter recovery and error propagation (Cross and Fleming, 1984). Decays were analyzed by a reconvolution procedure (Grinvald and Steinberg, 1974) using nonlinear least squares regression (Bevington, 1969). Joint support plane confidence intervals were calculated for all iterated parameters by an approximation method (Straume et al., 1991).

Molecular modeling

Molecular models of the GWO and GPW peptides were based on the atomic coordinates of the peptide [(Pro-Hyp-Gly)$_4$-Glu-Lys-Gly-(Pro-Hyp-Gly)$_5$]$_3$ (Berman et al., 2000, Kramer et al., 2000) (http://www.rcsb.org/pdb; PDB ID: 1QSU) and built using the molecular modeling software SYBYL 6.1 (Tripos Inc., St. Louis, MO) and Molecular Operating Environment 2000.02 (Chemical Computing Group Inc., Montreal, Canada). Excess residues (Pro-Hyp at the N-terminal and Gly-Pro-Hyp-Gly at the C-terminal) were removed and acetyl and amide groups were added at the N- and C-termini, respectively. The Glu-Lys sequence in the center was then substituted by Trp-Hyp to generate GWO and Pro-Trp to generate GPW. These structures were refined by energy minimization using Kollman's all-atom forcefield (Weiner et al., 1986).

The accessible side-chain conformations of Trp at a single X site of GWO or a single Y site of GPW were evaluated using the Random Incremental Pulse Search method (Ferguson and Raber, 1989) while holding fixed the sites of all other atoms; only a single Trp residue on peptide chain C was investigated in each trimer. Only side-chain conformations with energy within 5.0 kcal/mol of the global minimum for each structure were kept. The Random Incremental Pulse Search method generates new molecular conformations by randomly perturbing the position of each atom in the molecule by 1 Å and by rotating about single bonds. Generated conformers were minimized until their root mean square gradient was <0.01 kcal/mol. Two conformations were considered different if their energies differed by 0.01 kcal/mol and their atom positions exceeded the tolerance of 0.1 Å.

RESULTS

Previous circular dichroism studies (Persikov et al., 2000) indicate that peptides GWO and GPW are triple helical with melting temperatures of 31.9°C and 26.1°C, respectively.

The fraction of triple-helical GPW determined from ellipticity at 15°C was 0.95 and 0.99 at concentrations of 0.10 and 0.50 mg/mL, respectively (not shown). Thus, at the concentrations ($\geq$ 0.25 mg/mL) and temperature (15°C) used in the current study, GPW was >95% triple helix; the more stable GWO peptide would have a higher fraction of triple-helical conformation at these concentrations.

Steady-state spectra

Ultraviolet absorbance spectra of GWO and GPW were essentially indistinguishable and typical of aqueous Trp or NATA. Fluorescence excitation and emission spectra were also typical of aqueous Trp or NATA. The relative fluorescence quantum yield was slightly higher in GPW than in GWO; the ratio of quantum yields was 1.06 $\pm$ 0.02. The similarities in Trp absorption, excitation, and emission spectra indicate that the time-averaged local environments of the X and Y sites in the collagen triple helix have comparable polarity indicative of extensive contact with water.

Time-resolved emission decays

Fluorescence intensity decays for Trp in GWO and GPW were well fit by a double exponential decay model; parameters are shown in Table 1 for data obtained with 295-nm excitation. Decays in both peptides were dominated by a long lifetime of ~9 ns; a shorter lifetime of ~2.5–3 ns contributed only ~4–5% to the emission intensity. Although the number average lifetime was longer in GPW (7.74 ns) than in GWO (7.16 ns); the ratio of average lifetimes (1.08) was similar to the ratio of quantum yields (1.06). Identical intensity decay parameters for both GWO and GPW were also recovered with 280-nm excitation (not shown).

In the context of a rotamer model for Trp fluorescence (Szabo and Rayner, 1980; Ross et al., 1992; McLaughlin and Barkley, 1997) the predominance of the longer lifetime species suggests that the indole side chain at both X and Y sites within collagen is predominately constrained to a single conformation that isolates the indole ring from interaction with local quenching groups such as the amide bond (Chen et al., 1996). Small differences in the local mobility and/or orientation of indole side chains at the X and Y sites modulate quenching because both the long (τ_2) and the short (τ_1) lifetimes were slightly longer in GPW (9.1, 2.9 ns) than in GWO (8.4, 2.4 ns).

Stern-Volmer quenching

The solvent accessibility of Trp residues at X and Y sites was evaluated by iodide quenching of the steady-state fluorescence. Stern-Volmer quenching curves for both GWO and GPW were linear up to 0.4 M iodide (Fig. 1); all curves extrapolated to a value of F_o/F of 1 within experimental error. Quenching constants (K_{sv}) for GWO and GPW were 14.2 $\pm$ 0.7 M^{-1} and 11.0 $\pm$ 0.5 M^{-1}, respectively, giving bimolecular collisional quenching constants (k_q) of 1.75 $\pm$ 0.09 $\times$ 10^9 M^{-1} s^{-1} for GWO and 1.26 $\pm$ 0.06 $\times$ 10^9 M^{-1} s^{-1} for GPW. The difference between the collision rates for GWO and GPW suggests that the indole ring is slightly more accessible to solvent at the X site than at the Y site.

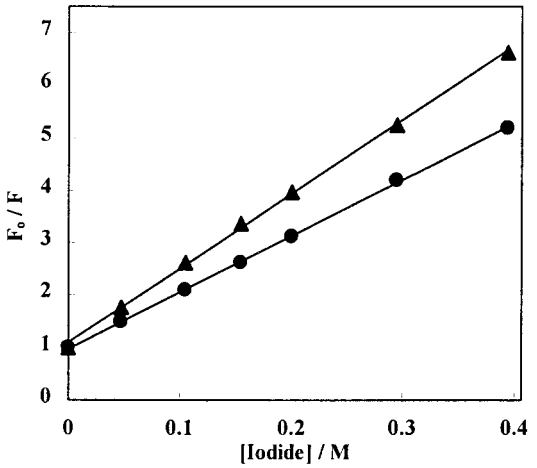

FIGURE 1 Stern-Volmer plot of the effect of quencher (iodide) on fluorescence intensity of the GWO (▲) and GPW (●) peptides. Error bars reflective of standard deviations are smaller than the symbols.

Steady-state anisotropy and the effect of solution viscosity

Depolarizing processes for Trp residues at the X and Y sites were initially assessed by steady-state anisotropy; with 280-nm excitation these values were 0.012 $\pm$ 0.003 for GWO and 0.032 $\pm$ 0.004 for GPW. Given the similarities in peptide size, shape, and fluorescence lifetime, this dramatic difference in anisotropy must reflect significant differences in the local mobility and/or orientation of the indole side chains at the X site compared to the Y site.

The effect of solution viscosity on the average rotational motion of Trp also differed considerably in the peptides. Perrin plots of the reciprocal of the steady-state anisotropy ($1/r$) versus the solution viscosity modulated by sucrose were linear over the full range of viscosities (Fig. 2). The linearity indicated that an analysis using a single rotational correlation time (ϕ) was appropriate for each peptide, despite the asymmetry of the triple helix (Steiner, 1991; Lakowicz, 1999). Apparent hydrodynamic volumes of the hydrated peptides (V_h) calculated from the Perrin Plots were 6.45 $\pm$ 0.68 nm^3 for GWO and 22.9 $\pm$ 3.0 nm^3 for GPW; these values are smaller than or comparable to the unhydrated volume of ~24 nm^3 calculated for a 26 residue polyproline-

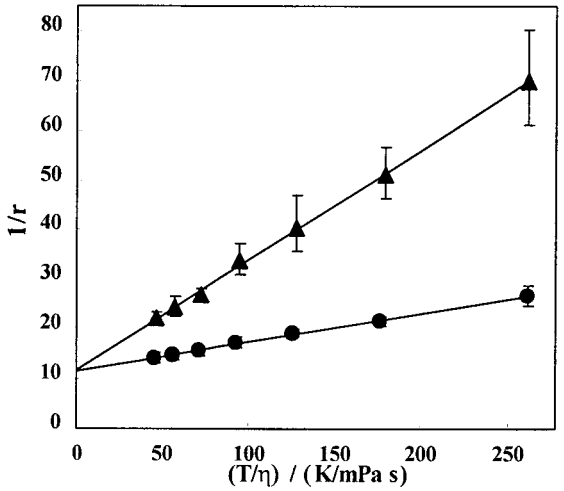

FIGURE 2 The effect of solution viscosity (varied by addition of sucrose) on the reciprocal of the steady-state anisotropy of the GWO (▲) and GPW (●) peptides. Error bars reflect the standard deviations; in some cases the error bars are smaller than the symbol.

like triple helix (assuming a 1-nm radius and 7.5-nm length; Bella et al., 1994). The extrapolated values of $1/r$ at infinite viscosity were 12.0 ± 0.6 for GWO and 11.8 ± 0.8 for GPW, giving r_o values of 0.083 and 0.085 for GWO and GPW, respectively, which are about half of the expected r_o value of Trp with 280-nm excitation (Eftink et al., 1990), suggesting that fast side-chain motions were unaffected by the viscosities used in the extrapolation.

There are two possible explanations for the dramatic differences in the steady-state anisotropy and apparent hydrodynamic volume of these peptides. First, the anisotropy may reflect differences in local mobility of Trp; the smaller anisotropy and apparent hydrodynamic volume of GWO would then reflect the additional fast motions of Trp residues at the X sites. Second, the anisotropy may reflect differences in the average orientation of the indole side chains with respect to the long axis of the asymmetric peptides; this would change the extent to which the depolarization reflects faster rotation about the long molecular axis or slower rotation about one of the two equivalent short molecular axes of the trimer. These two possibilities were investigated by time-resolved fluorescence anisotropy.

Time-resolved anisotropy

The limiting excitation anisotropy of Trp is wavelength dependent, increasing toward lower energy (Eftink et al., 1990). To enhance recovery of the fluorescence anisotropy decay parameters, excitation was at 295 nm. Two rotational correlation times were required to fit the GWO and GPW fluorescence anisotropy decays. All possible associations of the two lifetimes with the two correlation times were evaluated (Bialik et al., 1998; Rachofsky and Laws, 2000). The acceptance of an analysis for a particular model required excellent fits, represented by reduced χ^2 values (given in Table 1) and randomly distributed residuals and autocorrelation of residuals (not shown) for all three decays of an anisotropy dataset, as well as recovery of physically relevant decay parameters. For example, consideration of the trimer shapes of the collagen peptides required that rotational correlation times should be <50 ns. In addition, based on the photophysics of Trp and the excitation wavelength, all β_{ij} terms should be limited to the range of 0–0.4; consequently, the $r_{o,i}$ term for each emitting species must be ≤ 0.4.

The fluorescence anisotropy decay of both GWO and GPW could only be fit by one of the nine possible models for two lifetimes and two correlation times; it is noteworthy that the same model explained the data for both peptides. As shown by the β_{1j} values in Table 1, the small fraction of Trp species with the shorter lifetime was depolarized with a 10–12-ns correlation time as expected for overall rotational motion(s) of the peptide trimer. These species were not depolarized at all ($\beta_{11} = 0$) by motions yielding the 0.5-ns correlation time. The predominant, long-lifetime Trp species in both GWO and GPW were depolarized by both sets of motions (Table 1). However, the different β_{2j} values indicate a significant difference between GWO and GPW in the extent of depolarization by the slow and fast motions. The Trp residue in GWO was almost completely depolarized by the fast motions; due to the small β_{22} value for this species, the confidence limits for the long correlation time of GWO were large. In contrast, there was almost equal depolarization by the two sets of motions for the Trp residue in GPW. This difference in the extent of depolarization by fast and slow motions is reflected in the much lower steady-state anisotropy seen for GWO.

A unique physical picture emerges from this associative analysis. At both the X and Y sites, a small (10–15%) fraction of the Trp side chains are in an environment that (1) places them near a quenching group, giving a short lifetime, and (2) constrains local motions such that they are depolarized only by rigid body rotational motion. The majority (85–90%) of Trp side chains at both the X and Y sites, however, are in a quite different environment. These Trp residues have a longer lifetime, indicating they are not near a quenching group such as a peptide bond. However, this population exhibits a dramatic difference between the X and Y sites in the extent of fast side-chain depolarization, suggesting that the rapid rotational motions of the Trp residues possessing the longer lifetime at the X site are more unconstrained and thus able to adopt more conformations than the similar Trp population at the Y site. This difference in conformational mobility could help explain the slightly larger k_q value for iodide quenching at the X site.

Molecular modeling

Computational modeling studies investigated the possible side-chain orientations of Trp at the X and Y sites. Energy

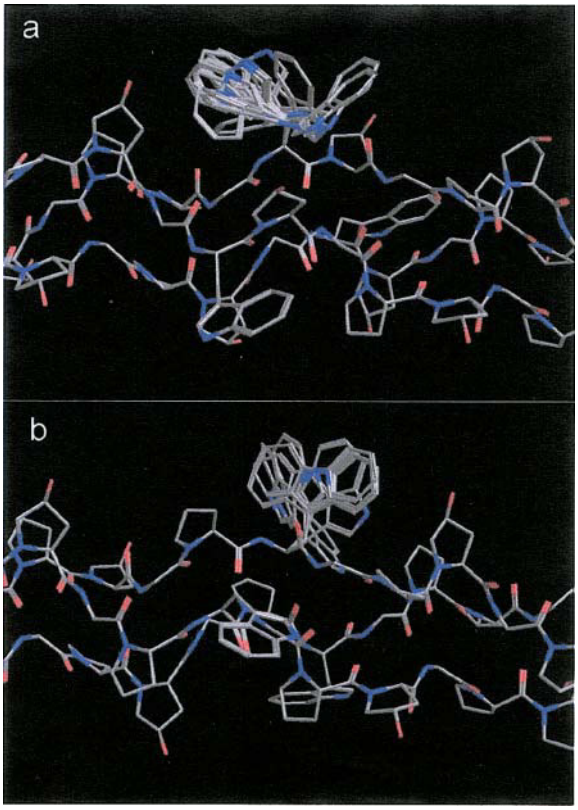

FIGURE 3 The accessible Trp side-chain conformations in (*a*) GWO and (*b*) GPW. All conformations with energy within 5 kcal/mol of the minimum are indicated.

minimized structures of both GWO and GPW in a water environment had rigid triple-helical backbone conformations whereas the side chains at both sites exhibited multiple conformations due to rotational freedom about both the C^{α}-C^{β} and C^{β}-C^{γ} bonds. A conformational search found 18 low energy Trp conformers in GWO (Fig. 3 *a*) and only nine conformers in GPW within the same energy cutoff (Fig. 3 *b*). The modeling results thus indicate that the Trp side chain has significantly more conformational freedom at the X than the Y site in the collagen triple helix, in agreement with the fluorescence anisotropy results.

Two of the conformers for GWO shown in Fig. 3 *a* are in a distinctly different orientation than the other 16. Careful examination of GPW conformers revealed one that has a distinctly different orientation than the other eight. The ratios of conformers agree with the ratios of amplitudes in the fluorescence intensity decays of both peptides (α_i, Table 1) and the conformer(s) associated with the smaller amplitude has the shorter lifetime. Furthermore, these conformers are the nearest to amide groups, which would explain their shorter fluorescence lifetimes (Chen et al., 1996). The close agreement between experiment and modeling suggests that in each peptide there are two distinct populations of indole side chains that do not interconvert on the nanosecond time scale, even though the larger population has significant dynamic motion sufficient to depolarize the excited state.

DISCUSSION

Side-chain flexibility, mobility, and the potential for multiple interactions are important for understanding the interaction of collagens with receptors, with other collagens, and with other matrix molecules. The binding of a monoclonal antibody to type III collagen (Shah et al., 1997), the recognition of the unique matrix metalloproteinase cleavage sites in fibrillar collagens (Fields, 1991), and the binding of heparin sulfate to the triple-helical domain of asymmetric acetylcholinesterase (Deprez et al., 2000), for example, all appear to involve triple-helical regions with low stability and, perhaps, excess mobility. NMR studies of labeled amino acids incorporated into collagen also show a high degree of side-chain and backbone mobility in fibrils (Batchelder et al., 1982). And high resolution x-ray structures of model peptides show side chains with multiple occupancies, indicating that side-chain conformational fluctuations can occur within crystals (Kramer et al., 2000). The novel approach presented here employs Trp fluorescence to compare the X and Y sites of collagen in solution, and has significantly expanded our understanding of side-chain environment and mobility in collagen.

Collagen side chains (except for Gly) are accessible to solvent and have little contact with potential protein quenching groups. The Stern-Volmer quenching results provide direct evidence that the indole ring is more accessible to solvent at the X than the Y site. This result supports and extends studies indicating that there are subtle but important differences between residues at the X and Y sites. For example, the large hydrophobic residues Leu, Phe, and Tyr are primarily found at the X site whereas Arg is predominantly at the Y site (Ramshaw et al., 1998), the C^{β} atom is exposed to solvent in the X but not the Y site in crystal structures of $(Pro\text{-}Pro\text{-}Gly)_{10}$ (Berisio et al., 2002), and molecular modeling studies suggest that residues in the X site are more available for interaction with other molecules than those in the Y site (Bansal, 1977; Bansal and Ramachandran, 1978).

Analysis of the fluorescence intensity decays amplifies our understanding of the solvent accessibility of collagen side chains. Trp fluorescence at each site is dominated by a lifetime of either 8.4 ns (X site) or 9.1 ns (Y site). These lifetimes are long for Trp in a protein (Beechem and Brand, 1985) and are similar to the lifetime of Trp amino acid at pH $\sim$11 where the α-amino group is unprotonated and thus a poor quencher (Beddard et al., 1980; Jameson and Weber, 1981), and to 3-methyl-indole in neutral aqueous solution (Beddard et al., 1980). The long lifetime in the collagen peptides is thus approximately equal to the maximum expected for an aqueous Trp and probably reflects the lifetime of hydrated indole not in contact with protein quenching groups. The short lifetime is

typical of the lifetime of aqueous NATA (3.2 ns; Lakowicz, 1999) or of Trp in a variety of proteins (Beechem and Brand, 1985) where the indole ring is close to the peptide bond quenching group (Chen et al., 1996). The lifetime characteristics of Trp in these two peptides indicates that it will be an excellent reporter group for the binding of collagen with various molecules (Kadler, 1994) because an interaction should force the Trp indole ring into closer proximity to protein quenching group(s) that will reduce the fluorescence lifetime.

Despite similarity in solvent accessibility, the dynamic behavior of Trp at the X and Y sites is remarkably dissimilar. The dramatic difference in steady-state anisotropy and apparent hydrodynamic volume between GWO and GPW, in which Trp residues with nearly identical lifetimes are in adjacent sites of nearly identical trimeric peptides, albeit remarkable, is easily understood by the considerable differences in the extent of rapid depolarizing motions at the X and Y sites. The anisotropy (either steady-state or time-resolved) should thus provide a sensitive signal for investigating the structural and dynamical consequences of amino acid variability both within and between chains in a triple helix. The mobility of Trp at an X site may be constrained by such interactions, with a concomitant increase in anisotropy, whereas the mobility of Trp at a Y site may be either more or less constrained by such interactions, with a concomitant increase or decrease in anisotropy.

It is possible that some of the fast depolarization seen in the time-resolved anisotropy results from resonance energy transfer between adjacent Trps (homotransfer) in the same peptide trimer (Demchenko, 1986). Although this possibility cannot be ruled out, it remains an unlikely explanation for two reasons. First, the distances between Trps in our models are 1.1–1.7 nm, significantly longer than the R_o of 0.5–0.7 nm estimated for Trp homotransfer (Eisinger et al., 1969). Second, homotransfer should depolarize both species, whereas only the longer lifetime species demonstrates rapid depolarization. The modeling results provide additional support for an interpretation based on rapid side-chain rotational motions.

Given the absolute requirement for Gly at every third site of the Gly-X-Y triplet, this study has probed all possible sites of amino acid variability within the essential folding motif of the most important vertebrate structural protein and established for the first time in solution that residues at X sites are not only more solvent accessible but also more mobile than residues at Y sites. It has been suggested that the more accessible X residues may be largely responsible for self-association as well as interactions with other molecules; it is possible that the extra mobility allows side chains at X sites to fluctuate among multiple interactions within fibrils, as seen in NMR studies of Leu (Batchelder et al., 1982). Further experiments will reveal the extent to which the side-chain mobility at the X and Y sites reflects local differences in side-chain packing inherent to the triple-helix structure and the extent to which side-chain mobility reflects differences in local flexibility due to the sequence of the triple helix.

This research was supported in part by funds from the Center for Advanced Food Technology, Rutgers University, to R.D.L., by National Institutes of Health (GM-60048) to B.B., by National Institutes of Health (HL-29019 and CA-63317) to J.B.A.R., by National Science Foundation (DBI-9724330) to W.R.L., and by a one-year Fellowship from the National Science Foundation to K.V.S.L.

REFERENCES

Badea, M., and L. Brand. 1979. Time-resolved fluorescence measurements. *In* Methods in Enzymology, Vol. 61. C. Hirs and S. Timasheff, editors. Academic Press, San Diego. 378–425.

Bansal, M. 1977. Stereochemical restrictions on the occurrence of amino acid residues in the collagen structure. *Int. J. Pept. Protein Res.* 9:224–234.

Bansal, M., and G. N. Ramachandran. 1978. A theoretical study of the structures of $(Gly\text{-}Pro\text{-}Leu)_n$ and $(Gly\text{-}Leu\text{-}Pro)_n$. *Int. J. Pept. Protein Res.* 11:73–81.

Batchelder, L. S., C. E. Sullivan, L. W. Jelinski, and D. A. Torchia. 1982. Characterization of leucine side chain reorientation in collagen fibrils by solid-state 2-H NMR. *Proc. Natl. Acad. Sci. USA.* 79:386–389.

Baum, J., and B. Brodsky. 1999. Folding of peptide models of collagen and misfolding in disease. *Curr. Opin. Struct. Biol.* 9:122–128.

Beddard, G., G. Fleming, G. Porter, and R. Robbins. 1980. Time-resolved fluorescence from biological systems: tryptophan and simple peptides. *Philos. Trans. R. Soc. London. Ser. A.* 298:321–334.

Beechem, J., and L. Brand. 1985. Time-resolved fluorescence of proteins. *Annu. Rev. Biochem.* 54:43–71.

Bella, J., M. Eaton, B. Brodsky, and H. M. Berman. 1994. Crystal and molecular structure of a collagen-like peptide at 1.9 Å resolution. *Science.* 266:75–81.

Berisio, R., L. Vitagliano, L. Mazzarella, and A. Zagari. 2002. Crystal structure of the collagen triple helix model $[(Pro\text{-}Pro\text{-}Gly)_{10}]^3$. *Protein Sci.* 11:262–270.

Berman, H. M., J. Westbrook, Z. Feng, G. Gilliland, T. N. Bhat, H. Weissig, and I. N. Shindyalov. 2000. The protein data bank. *Nucleic Acids Res.* 28:235–242.

Bevington, P. R. 1969. Data Reduction and Error Analysis for the Physical Sciences. McGraw-Hill, New York.

Bialik, C., B. Wolf, E. Rachofsky, J. B. A. Ross, and W. R. Laws. 1998. Dynamics of biomolecules: assignment of local motions by fluorescence anisotropy decay. *Biophys. J.* 75:2564–2573.

Buevich, A. V., and J. Baum. 2001. Nuclear magnetic resonance characterization of peptide models of collagen-folding diseases. *Philos. Trans. R. Soc. London. Ser. B.* 356:159–168.

Chen, Y., B. Liu, H. T. Yu, and M. Barkley. 1996. The peptide bond quenches indole fluorescence. *J. Am. Chem. Soc.* 118:9271–9278.

Cross, A. J., and G. R. Fleming. 1984. Analysis of time-resolved fluorescence anisotropy decays. *Biophys. J.* 46:45–56.

Demchenko, A. 1986. Ultraviolet Spectroscopy of Proteins. Springer-Verlag, Berlin.

Deprez, P., E. Doss-Pepe, B. Brodsky, and N. C. Inestrosa. 2000. Interaction of the collagen-like tail of asymmetric acetylcholiesterase with heparin depends on triple-helical conformation, sequence, and stability. *Biochem. J.* 350:283–290.

Edelhoch, H. 1967. Spectroscopic determination of tryptophan and tyrosine in proteins. *Biochemistry.* 6:1948–1954.

Eftink, M. R., L. A. Selvidge, P. R. Callis, and A. A. Rehms. 1990. Photophysics of indole derivatives: experimental resolution of ^1L_a and ^1L_b transitions and comparison with theory. *J. Phys. Chem.* 94:3469–3479.

Eisinger, J., B. Feurer, and A. Lamola. 1969. Intramolecular singlet energy transfer: applications to peptides. *Biochemistry*. 8:3908–3915.

Ferguson, D. M., and D. J. Raber. 1989. An approach to probing conformational space with molecular mechanics: random incremental pulse search. *J. Am. Chem. Soc*. 111:4371–4378.

Fields, G. B. 1991. A model for interstitial collagen catabolism by mammalian collagenases. *J. Theor. Biol*. 153:585–602.

Fujimori, E. 1966. Ultraviolet light irradiated collagen macromolecules. *Biochemistry*. 5:1034–1040.

Golbik, R., J. Eble, A. Ries, and K. Kuhn. 2000. The spatial orientation of the essential amino acid residues arginine and aspartate within the $\alpha 1\beta 1$ integrin recognition site of collagen IV has been resolved using fluorescence resonance energy transfer. *J. Mol. Biol*. 297:501–509.

Grinvald, A., and I. Z. Steinberg. 1974. On the analysis of fluorescence decay kinetics by the method of least squares. *Anal. Biochem*. 59:583–598.

Hoppe, H.-J., and K. B. M. Reid. 1994. Collectins—soluble proteins containing collagenous regions and lectin domains—and their roles in innate immunity. *Protein Sci*. 3:1143–1158.

Jameson, D., and G. Weber. 1981. Resolution of the pH-dependent heterogeneous fluorescence decay of tryptophan by phase and modulation measurements. *J. Phys. Chem*. 85:953–958.

Jones, E. Y., and A. Miller. 1991. Analysis of structural design features in collagen. *J. Mol. Biol*. 218:209–219.

Kadler, K. 1994. Extracellular matrix 1: fibril-forming collagens. *Protein Profile*. 1:519–638.

Kielty, C. M., I. Hopkinson, and M. E. Grant. 1993. The collagen family: structure, assembly and organization in the extracellular matrix. *In* Connective Tissue and its Heritable Disorders: Molecular, Genetic and Medical Aspects. P. M. Royce and B. Steinmann, editors. Wiley Liss, New York. 103–148.

Kramer, R. Z., M. G. Venugopal, J. Bella, P. Mayville, B. Brodsky, and H. M. Berman. 2000. Staggered molecular packing in crystals of a collagen-like peptide with a single charged pair. *J. Mol. Biol*. 301:1191–1205.

Kramer, R. Z., J. Bella, B. Brodsky, and H. M. Berman. 2001. The crystal and molecular structure of a collagen-like peptide with a biologically relevant sequence. *J. Mol. Biol*. 311:131–147.

Lakowicz, J. R. 1999. Principles of Fluorescence Spectroscopy. Kluwer Academic/Plenum, New York.

McLaughlin, M., and M. Barkley. 1997. Fluorescence spectroscopy. *In* Methods in Enzymology. Vol. 278. L. Brand and M. Johnson, editors. Academic Press, San Diego. 190–202.

Menter, J. M., G. D. Williamson, K. Carlyle, and I. Willis. 1995. Photochemistry of type I acid-soluble calf skin collagen: dependence on excitation wavelength. *Photochem. Photobiol*. 62:402–408.

Muller, J. C. D., J. Ottl, and L. Moroder. 2000. Hereotrimeric collagen peptides as fluorogenic collagenase substrates: synthesis, conformational properties, and enzymatic digestion. *Biochemistry*. 39:5111–5116.

Persikov, A. V., J. A. M. Ramshaw, A. Kirkpatrick, and B. Brodsky. 2000. Amino acid propensities for the collagen triple-helix. *Biochemistry*. 39:14960–14967.

Rachofsky, E. L., and W. R. Laws. 2000. Kinetic models and data analysis methods for fluorescence anisotropy decay. *In* Methods in Enzymology. Vol. 321. M. L. Johnson and L. Brand, editors. Academic Press, San Diego. 216–238.

Ramshaw, J. A. M., N. K. Shah, and B. Brodsky. 1998. Gly-X-Y tripeptide frequencies in collagen: a context for host-guest triple-helical peptides. *J. Struct. Biol*. 122:86–91.

Rich, A., and F. H. C. Crick. 1961. The molecular structure of collagen. *J. Mol. Biol*. 3:483–506.

Ross, J. B. A., H. R. Wyssbrod, R. A. Porter, C. A. Schwartz, C. A. Michaels, and W. R. Laws. 1992. Correlation of tryptophan fluorescence intensity decay parameters with proton NMR-determined rotamer conformations:[tryptophan$_2$]oxytocin. *Biochemistry*. 31:1585–1594.

Sell, D. R., R. H. Nagaraj, S. K. Grandhee, P. Odetti, A. Lapolla, J. Fogarty, and V. M. Monnier. 1991. Pentosidine: a molecular marker for the cumulative damage to proteins in diabetes, aging, and uremia. *Diabetes Metab. Rev*. 7:239–251.

Shah, N. K., M. Sharma, A. Kirkpatrick, J. A. M. Ramshaw, and B. Brodsky. 1997. Gly-gly-containing triplets of low stability adjacent to a type III collagen epitope. *Biochemistry*. 36:5878–5883.

Steiner, R. F. 1991. Fluorescence anisotropy: theory and applications. *In* Topics in Fluorescence Spectroscopy. Vol. 2. J. R. Lakowicz, editor. Plenum Press, New York. 1–52.

Straume, M., S. G. Frasier-Cadoret, and M. L. Johnson. 1991. Least-squares analysis of fluorescence data. *In* Topics in Fluorescence Spectroscopy, Vol. 2. J. R. Lakowicz, editor. Plenum, New York. 177–240.

Szabo, A., and D. Rayner. 1980. Fluorescence decay of tryptophan conformers in aqueous solution. *J. Am. Chem. Soc*. 102:554–563.

Uebelhart, D., and P. D. Delmas. 1993. The determination of collagen crosslinks in the study of bone and cartilage degradation. *Pathol. Biol*. 41:951–961.

Waxman, E., W. R. Laws, T. M. Laue, Y. Nemerson, and J. B. A. Ross. 1993. Human factor VIIa and its complex with soluble tissue factor: evaluation of asymmetry and conformational dynamics by ultracentrifugation and fluorescence anisotropy decay methods. *Biochemistry*. 32:3005–3012.

Weiner, S. J., P. A. Kollman, D. T. Nguyen, and D. A. Case. 1986. An all atom forcefield for simulations of proteins and nucleic acids. *J. Comp. Chem*. 7:230–252.